Supplement of Atmos. Chem. Phys., 26, 16477–16500, 2026
https://doi.org/10.5194/acp-26-16477-2026-supplement
© Author(s) 2026. CC BY 4.0 License.



Atmospheric Chemistry and Physics
Open Access

Supplement of

Molecular composition of wintertime haze over the northern Indian Ocean suggests extensive atmospheric processing during transport

Karin Stegelius et al.

Correspondence to: Krishnakant Budhavant (kbbudhavant@gmail.com) and Sophie L. Haslett (sophie.haslett@aces.su.se)

The copyright of individual parts of the supplement might differ from the article licence.

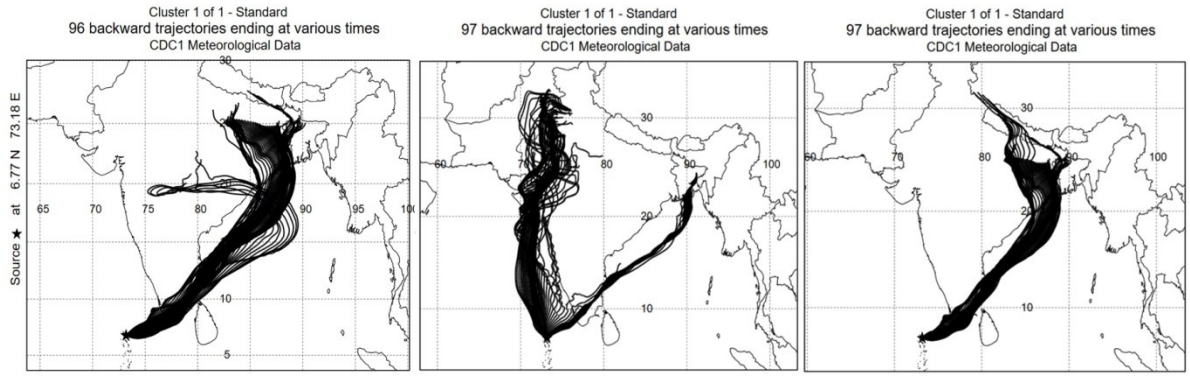


Figure S1: 10-day back trajectories generated hourly for period 1 (15–19 January 08:00–08:00(MVT)), period 2 (30 January–3 February 09:00–09:00(MVT)) and period 3 (14–18 February 06:00–06:00(MVT))

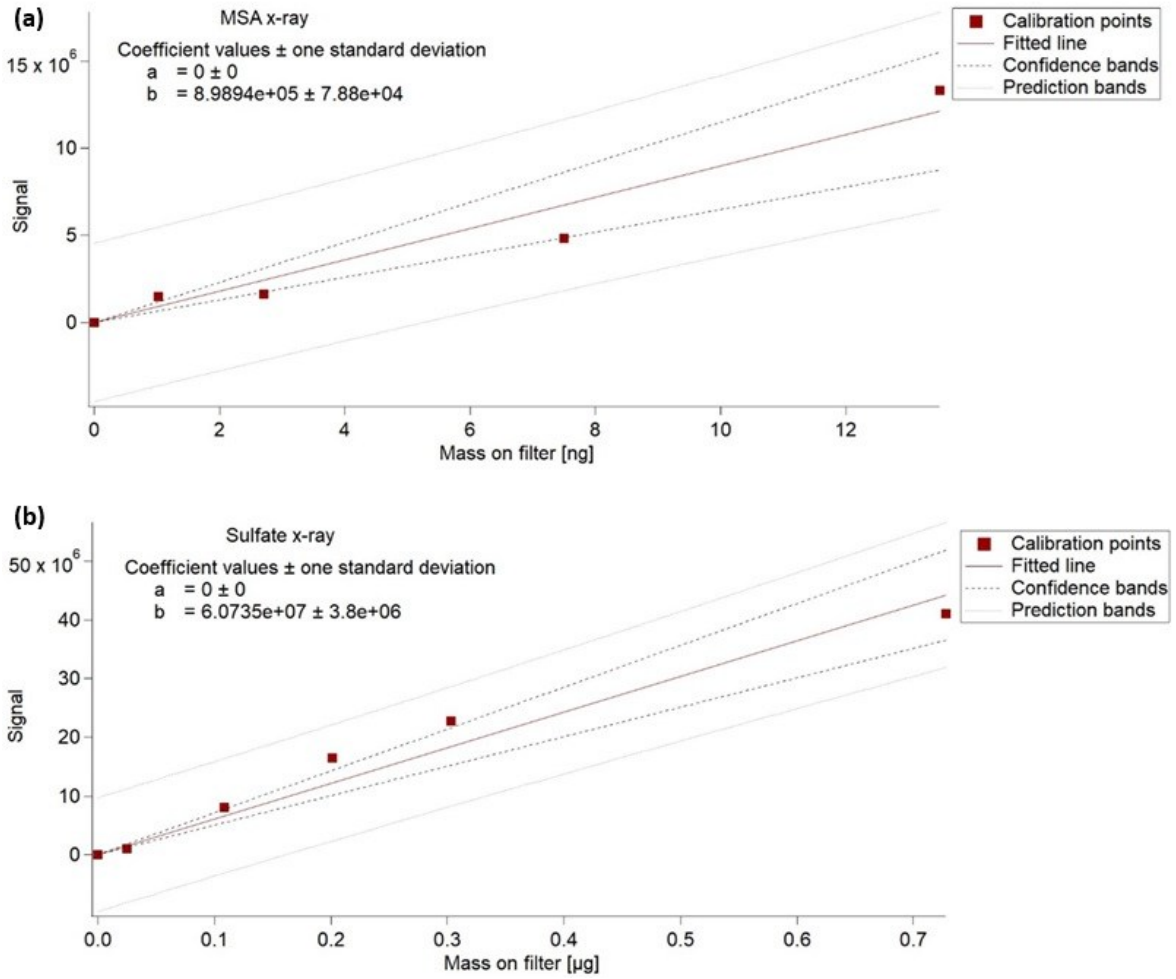


Figure S2: The calibration curves for (a) MSA using a x-ray source and (b) Sulfate represented by the peak of SO3-I using a x-ray source, the red squares are the calibration points, the red line the calculated straight line when forced through zero, the black dotted line are the confidence band (within which model points are expected to fall) and the light grey dotted line are prediction band (within which measured points are expected to fall) for a 95% confidence interval. In addition, the coefficient values for the fitted line are also displayed. A two-tailed t-test (alfa 0.05) showed that the intercept was non- significant for the MSA case and for the sulfate case it was a close call, why the decision was made to calculate both calibration curves with the line forced through zero.

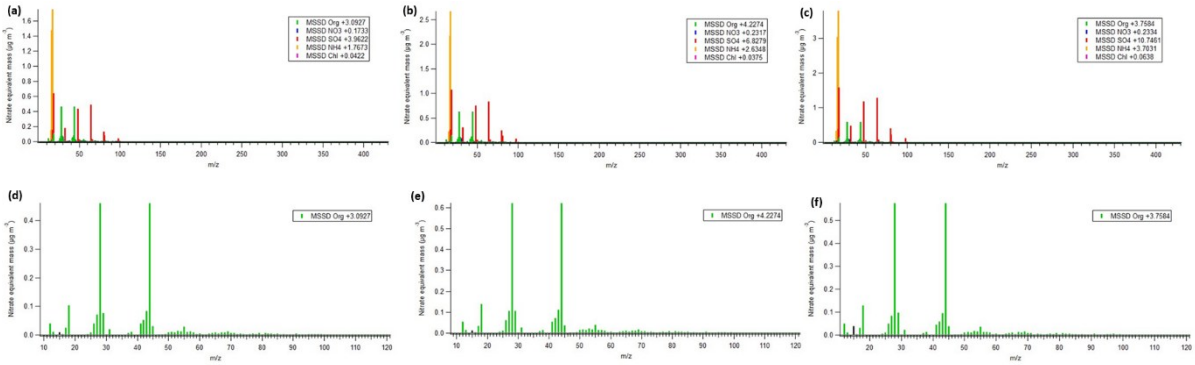


Figure S3: Mass spectra for all species observed with the AMS; Org, NO_3, SO_4, NH_4 and Chl during the three different time periods (a) period 1, (b) period 2 and (c) period 3 and the mass spectra for the organics only during (d) period 1, (e) period 2 and (f) period 3.

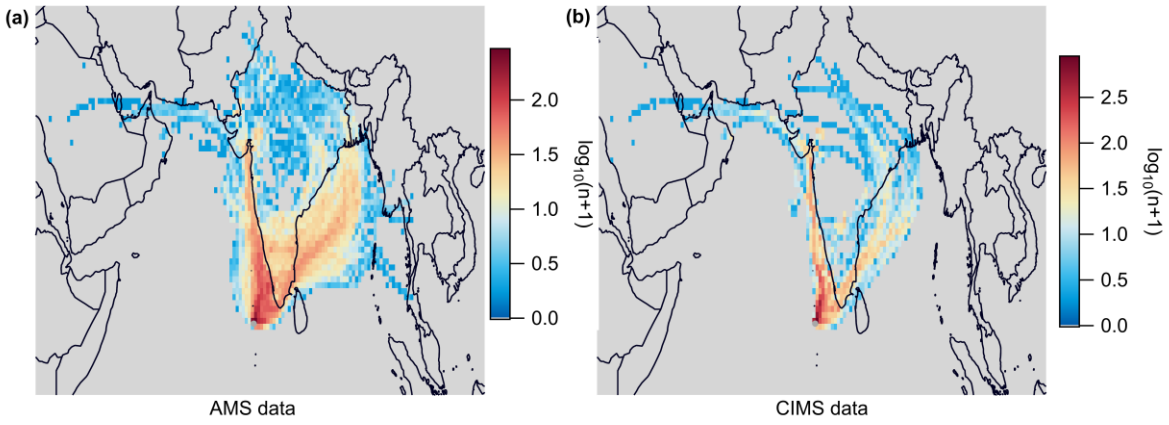


Figure S4: Trajectory density for concentration-weighted back trajectory analyses carried out using (a) AMS data and (b) CIMS data.

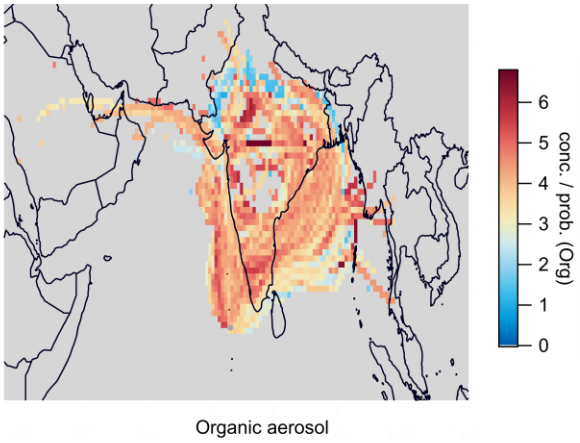


Figure S5: Concentration-weighted back trajectory for organic aerosol, as measured by the AMS.

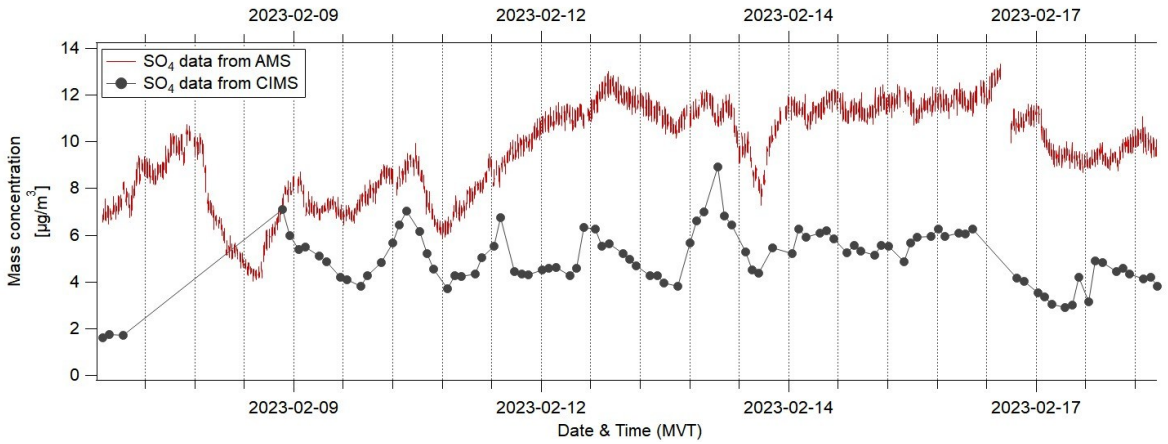


Figure S6: Time series of SO_4 data from AMS (red) and CIMS (black) during the time period 7 – 18 February 2023. The mass concentration from the CIMS is derived from calibration of the SO_3-I peak and converted from mass to a mass concentration by accounting for the flow rate and collection time at sampling, as described in section 2.4 in the main text.

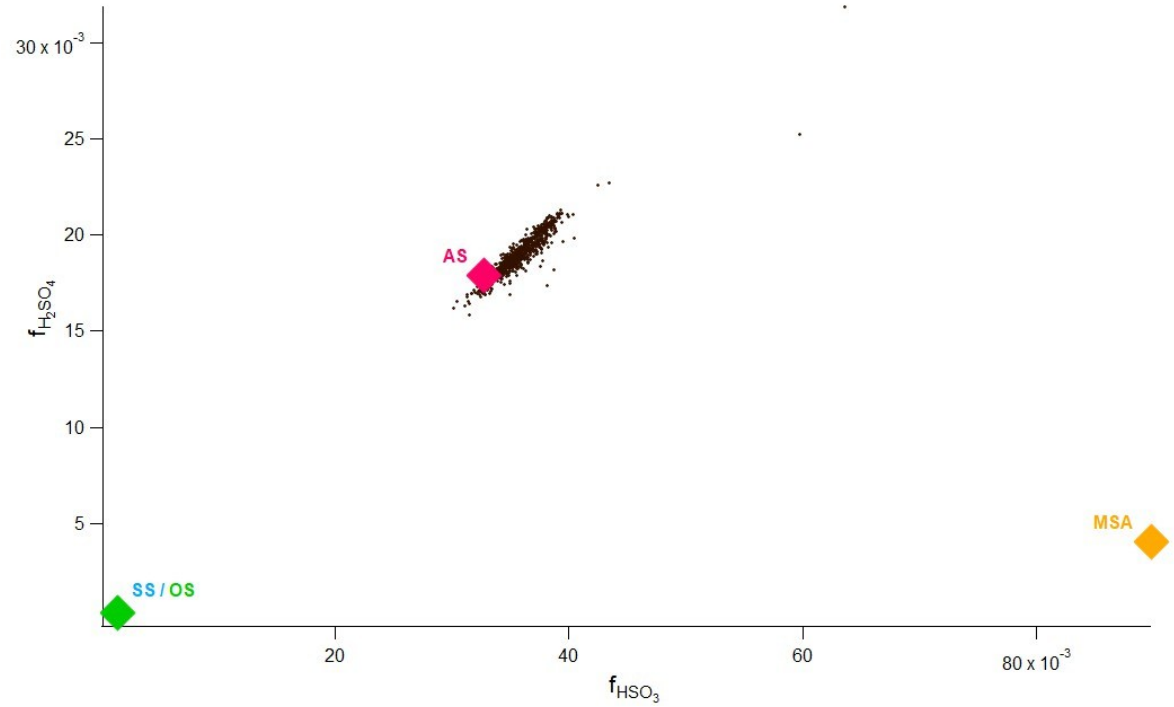


Figure S7: The fraction of $H_2SO_4^+$ (f_{H2SO4}) and HSO_3^+ (f_{HSO3}) to total SO_4 (i.e SO^+ (m/z 48) + SO_2^+ (m/z 64) + SO_3^+ (m/z 80) + HSO_3^+ (m/z 81) + $H_2SO_4^+$ (m/z 98)) observed with the AMS for 4 standard compounds, Ammonium sulfate (AS), Methane sulfonic acid (MSA), Organo sulfate (OS) and Sodium sulfate (SS). The black dots show hourly averaged f_{HSO3} and f_{H2SO4} for all measured SO_4 during the campaign at MCOH.

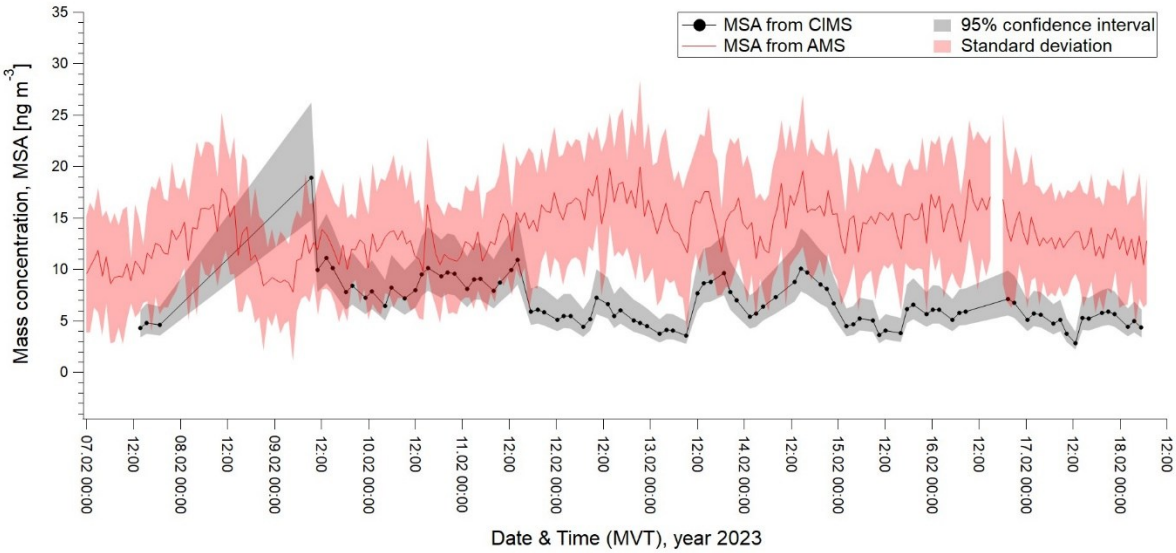


Figure S8: Time series of the MSA mass concentration (in ng m^{-3}) calculated from AMS and CIMS data during the time period 7 – 18 February 2023. Data points from the AMS, shown by the red line, are hourly averaged and the standard deviation is displayed by the shaded area. Data from the CIMS are shown in black, with a shaded grey region to display the upper and lower mass concentrations based on the 95% confidence interval for the signal value in the sensitivity calibration.

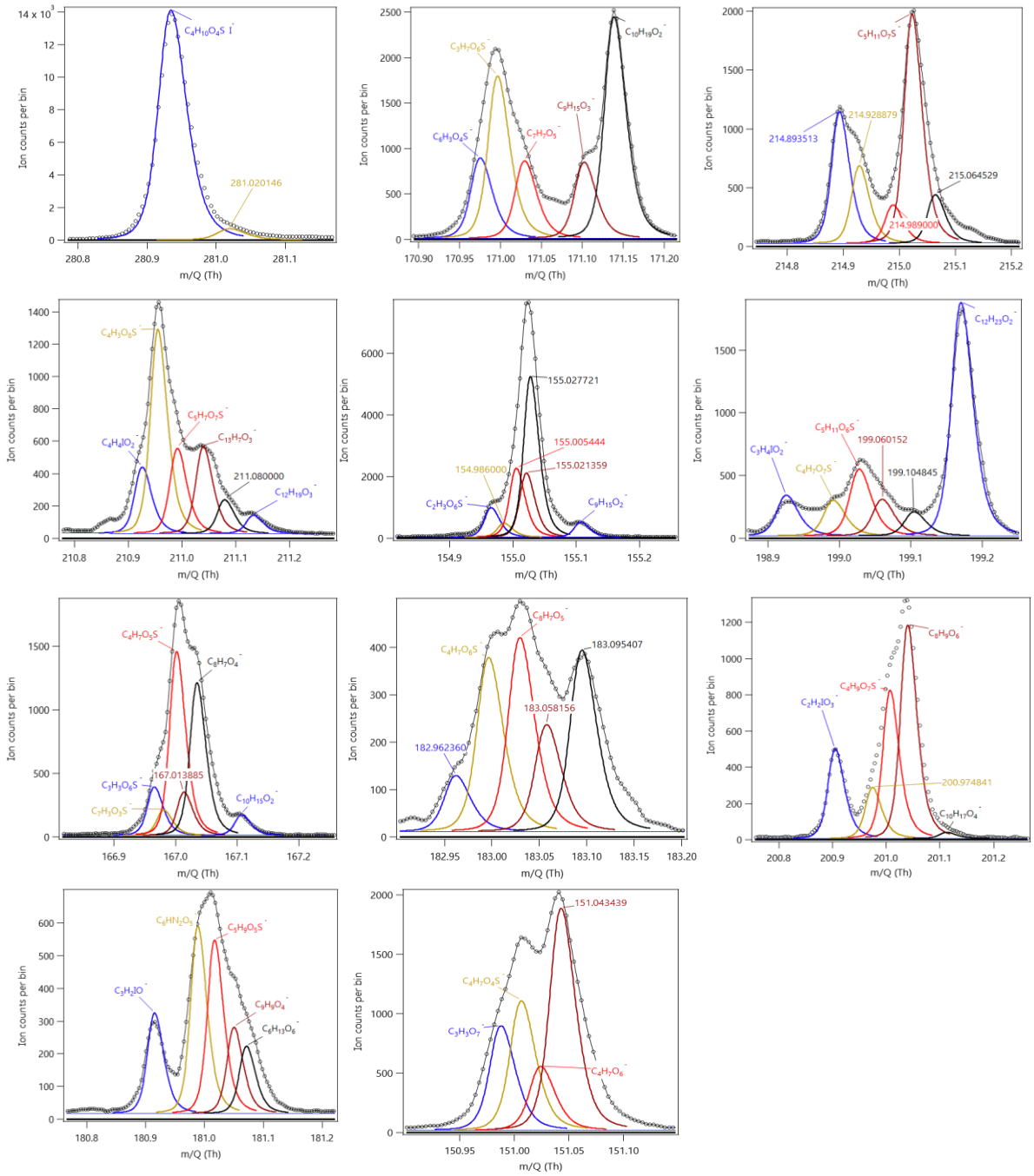


Figure S9: Peak fits for the sulfur-containing organic compound signals observed by the CIMS

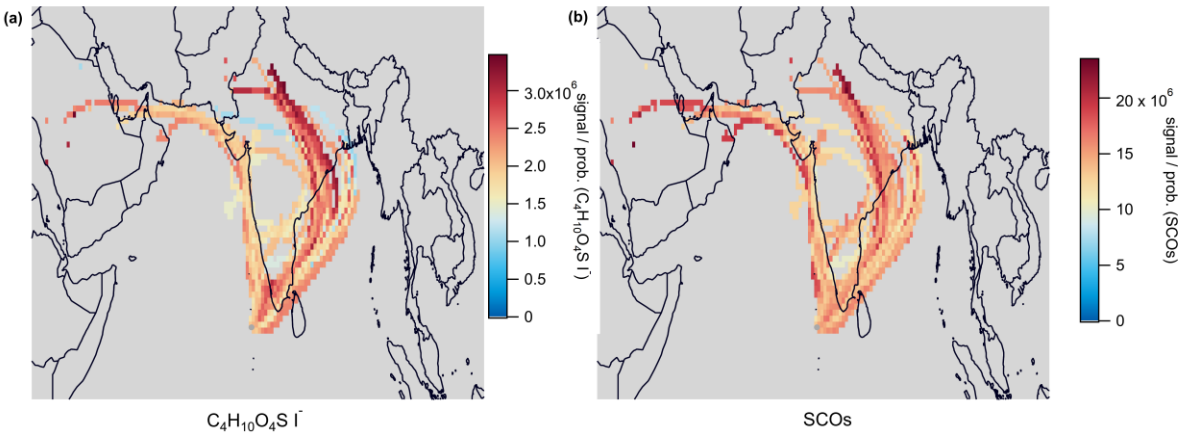


Figure S10: Concentration-weighted back trajectories for (a) the CIMS signal at $C_4H_{10}O_4S\ I^-$ and (b) the sum of the signals at $C_4H_9O_5S^-$, $C_4H_7O_6S^-$, $C_4H_7O_7S^-$, $C_4H_9O_7S^-$, $C_4H_3O_8S^-$, $C_5H_9O_5S^-$, $C_5H_{11}O_6S^-$, and $C_5H_7O_7S^-$..

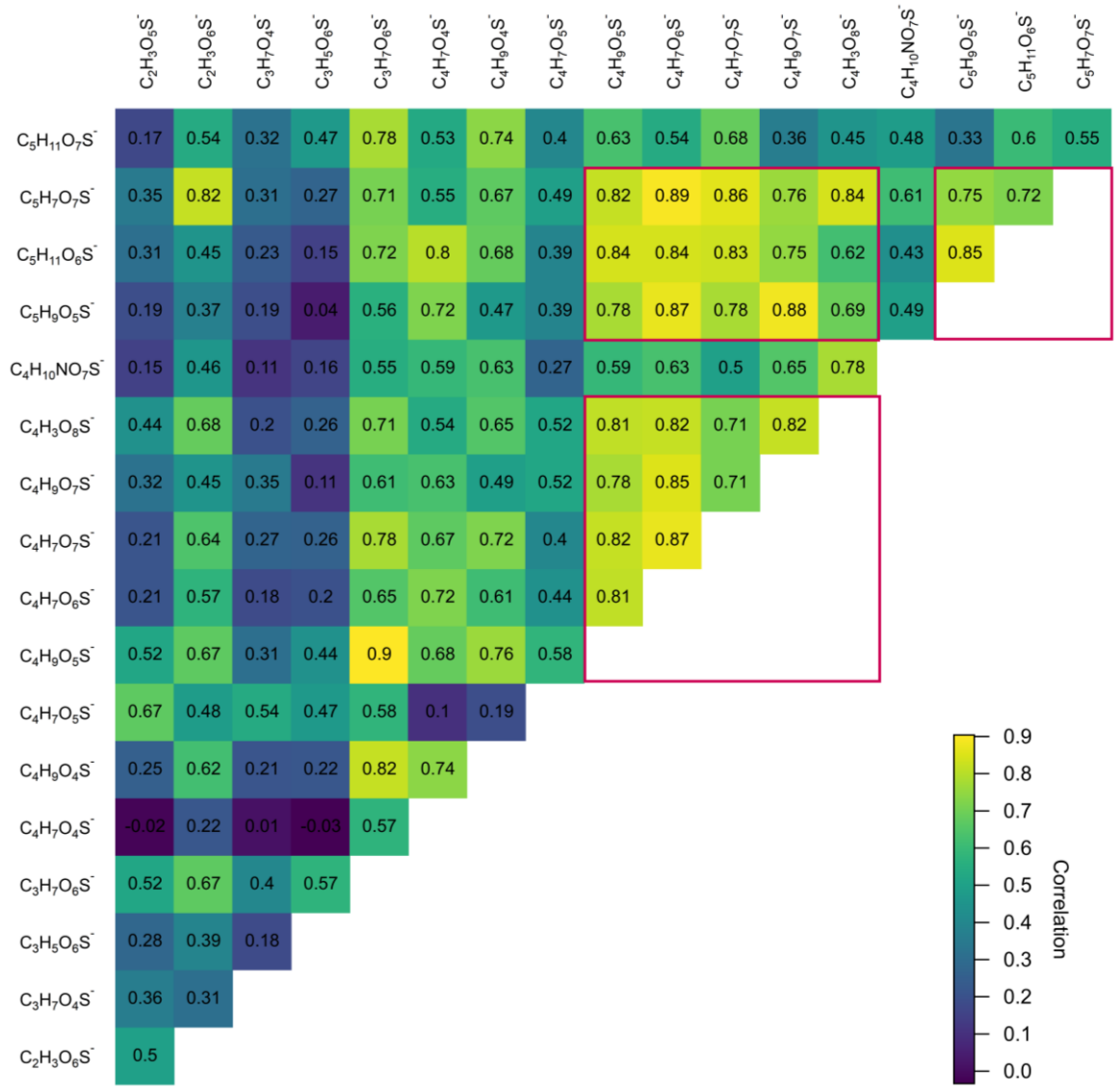


Figure S11: Correlation matrix for the SCOs identified in Table 2. The correlation between two identified compounds is shown both by the colour of the box and the printed number. The red boxes represent the eight highly-correlated signals that are combined to create the concentration-weighted back trajectory plot shown in Fig. S9.

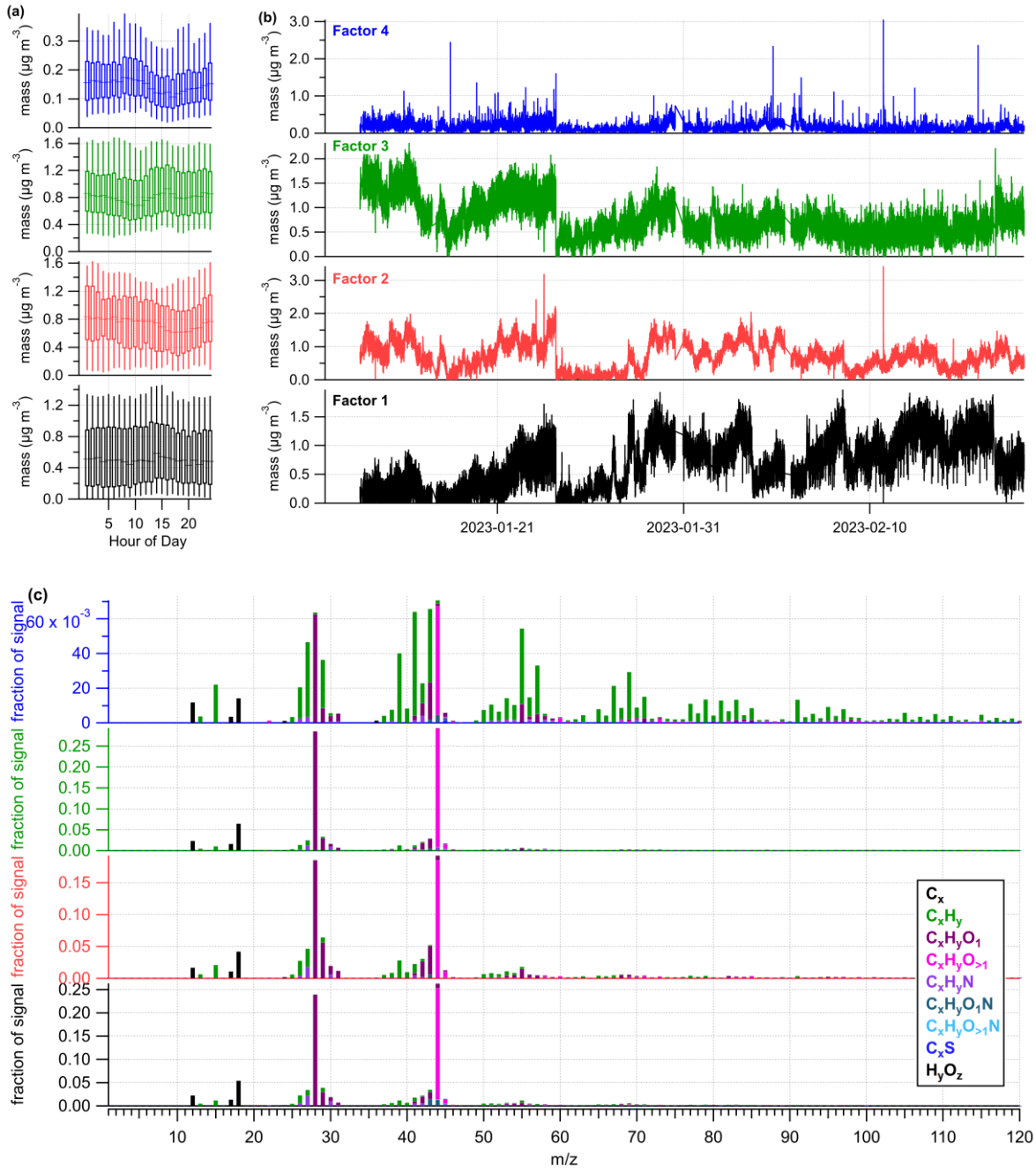


Figure S12: Four-factor PMF results for the organic aerosol observed by the AMS: (a) diel cycles, (b) time series, and (c) mass spectra. For the results presented in the main text, factors 1–3 are merged into one LV-OOA factor.

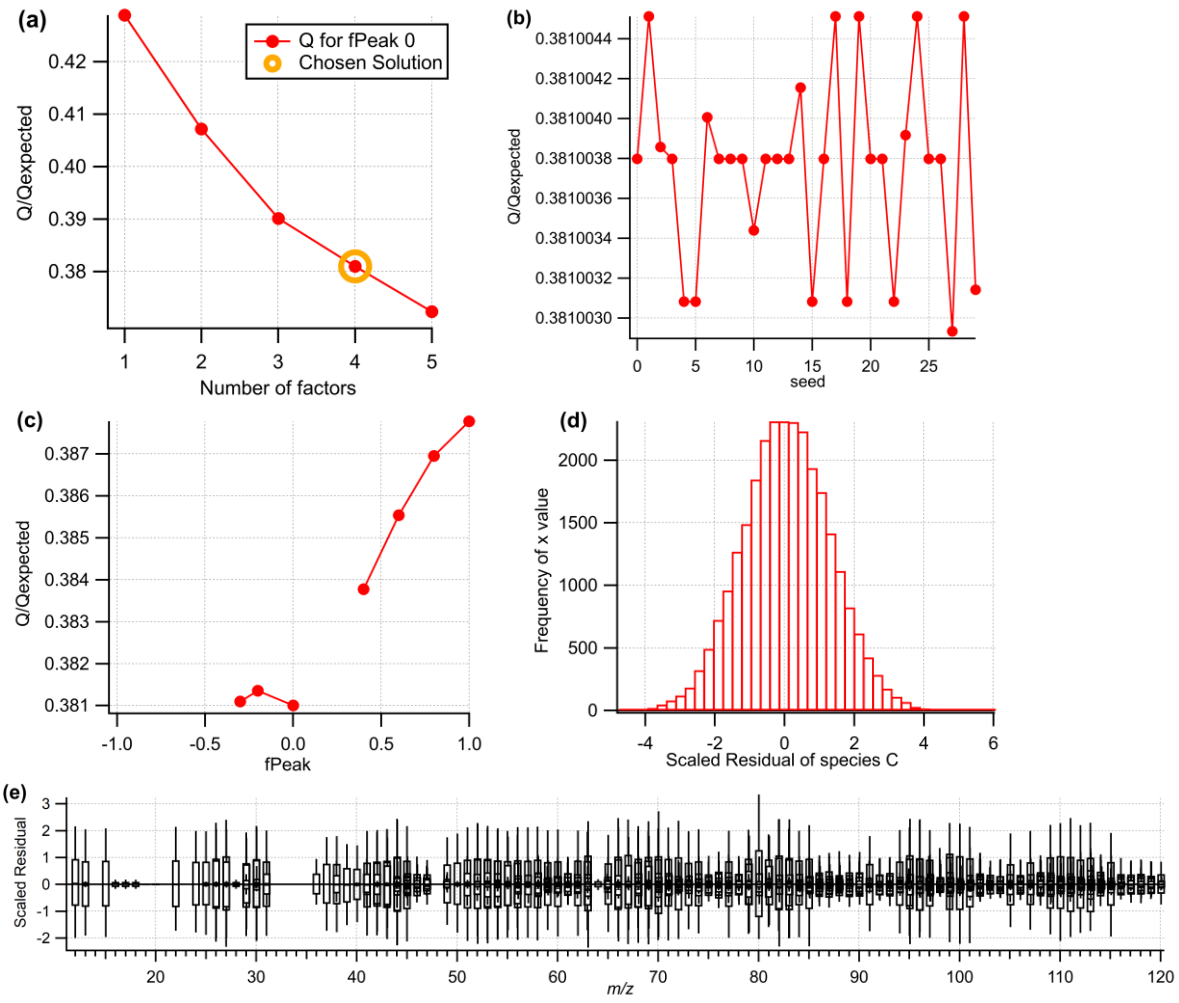


Figure S13: (a) Q/Q_{exp} for the 1 to 5 factor solutions, (b) Q/Q_{exp} across 30 seeds for the four-factor solution, (c) Q/Q_{exp} for different fPeak rotations for the four-factor solution, (d) scaled residuals, and (c) box plots of scaled residuals for each *m/z*.

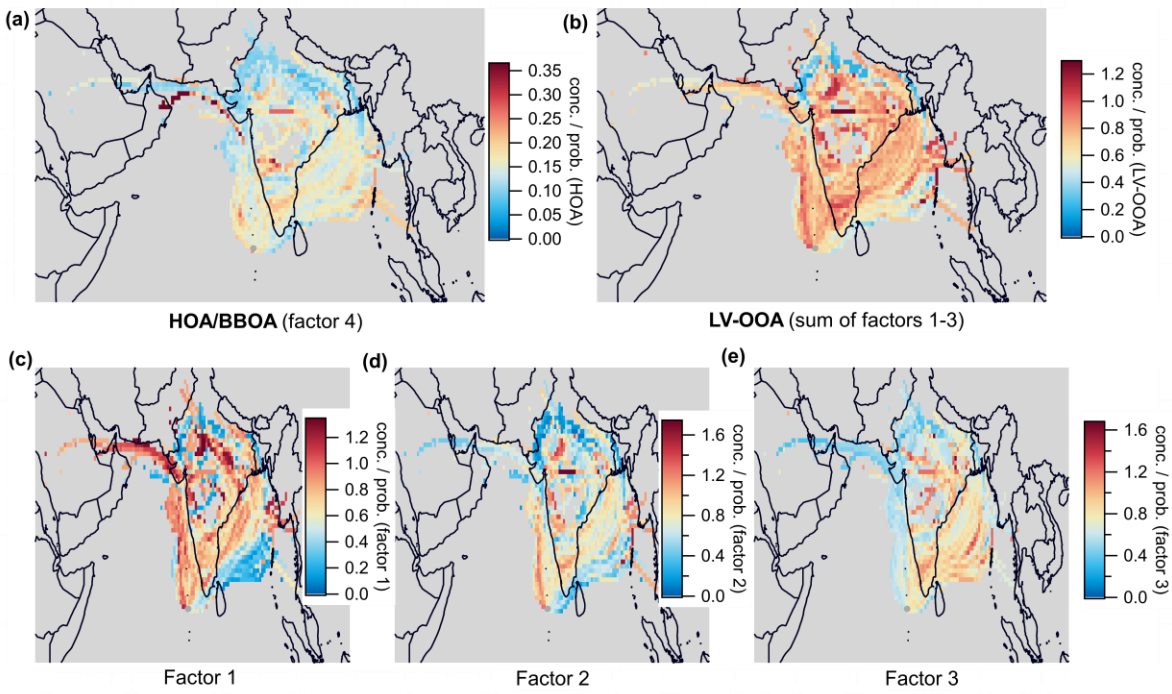


Figure S14: Concentration-weighted back trajectory analysis for (a) the HOA/BBOA factor, (b) the merged LV-OOA factor, and the individual LV-OOA factors, (c) factor 1, (d) factor 2, (e) factor 3.

Text S1: Ion balance

A rough ion balance, using the approach outlined by Zhang et al. (2007), gives the following result as a campaign average:

$$\frac{NH_4(measured)}{NH_4(neutralised)} = \frac{\frac{NH_4}{18}}{2 \times \frac{SO_4}{96} + \frac{NO_3}{62} + \frac{Chl}{35.5}} = \frac{\frac{2.54}{18}}{2 \times \frac{6.49}{96} + \frac{0.181}{62} + \frac{0.0419}{35.5}} \approx \mathbf{1.01}$$

Here, *NH₄ (measured)* refers to measured NH_4 ions, while *NH₄* (neutralised) refers to the ammonium (*NH₄*) ions that would be required to neutralise all of the observed sulfate (*SO₄*), nitrate (*NO₃*), and chloride (*Chl*) ions. A value substantially lower than 1 indicates that there is not enough NH_4 available to neutralise the cations, suggesting a more acidic aerosol. However, a value close to unity, as is seen here, indicates a neutral aerosol.

References

Zhang, Q., Jimenez, J. L., Worsnop, D. R., and Canagaratna, M.: A Case Study of Urban Particle Acidity and Its Influence on Secondary Organic Aerosol, Environ. Sci. Technol., 41, 3213–3219, https://doi.org/10.1021/es061812j, 2007.